J|A|C|S ARTICLES

Published on Web 08/03/2009

Porphyrin Arrays Responsive to Additives. Fluorescence Tuning

Takeshi Yamamura,*,† Shingo Suzuki,† Tomotaka Taguchi,† Akira Onoda,‡ Toshiaki Kamachi,§ and Ichiro Okura⊥

Department of Chemistry, Faculty of Science, Science University of Tokyo, Kagurazaka, Shinjuku-ku, Tokyo 162-0825, Japan, Department of Applied Chemistry, Graduate School of Engineering, Osaka University, 2-1 Yamadaoka, Suita, Osaka 565-0871, Japan, Department of Molecular Design and Engineering, Graduate School of Engineering, Nagoya University, Chikusa, Nagoya 464-8603, Japan, and Department of Bioscience and Biotechnology, Tokyo Institute of Technology, 4259 Nagatsuta-cho, Midori-ku, Yokohama-shi, Kanagawa Pref. 226-8501, Japan

Received December 20, 2008; E-mail: tyamamur@rs.kagu.tus.ac.jp

Abstract: The application of low-flux sunlight begins with the synthesis of effective antenna systems. This requires the development of dye integrates with optimized dye orientation for effective energy transfer. We here report a series of peptide-linked porphyrin arrays, denoted by Boc−$(Por^{Zn,S})_n$−OBu^t ($n = 2$, 4, and 8), that change their dye orientation to increase fluorescence responsively to additive reagents. The B-band absorption (AB) regions of the arrays show blue shifts (dimer, 407.6 nm; tetramer, 408.2 nm; octamer, 407.8 nm) in organic solvents as compared to that of Boc−$Por^{Zn,S}$−OBu^t (monomer, 422.6 nm) and the fluorescence yield Φ' of the arrays decreases with increasing n, obeying the relationship $\Phi' = 0.03/n^{1.5}$; however, the arrays are tuned up in fluorescence emission by the addition of 1,2-diaminoethane (en). The addition of a sufficient amount of en increases the fluorescence of the porphyrins in monomer, dimer, tetramer, and octamer by ∼5, ∼12, ∼12, and >730 times, respectively, when compared with that observed in the absence of en. This also causes asymptotic red shifts in absorption (AB) bands (B-band λ_{max}: 410 to 429−430 nm), as well as changes in circular dichroism (CD) spectra, and makes porphyrins approach new mutual asymmetric orientations. Our results show the potentiality of the tunable dye polymers that are *a posteriori* optimized in dye orientation and fluorescence emission by additive reagents for the development of effective light-harvesting materials.

1. Introduction

The application of low-flux sunlight begins with the synthesis of effective antenna systems. This requires the development of dye integrates equipped with optimized dye orientation for effective energy transfer. However, photon energies absorbed in integrated dye systems are easily lost through thermal quenching when the mutual orientations of the dyes are unsuitable for energy transfer. Therefore, it is required to develop dye integrates that achieve optimal orientations for effective energy transfer. Antenna chlorophylls (Chls) observed in LH1,[1] LH2,[2] chlorosomes,[3,4] green plants,[5] and cyanobacteria,[6] as well as that of Fenna−Matthews−Olson (FMO)[7] proteins, are good solutions to this orientation control problem. Among these natural systems, LH1 and LH2 were the first systems mimicked by chemists for the synthesis of artificial light-harvesting systems. The beautiful arrangement of Chls observed in these systems led to the introduction of $\pi-\pi$ stacked and flat-ring arrays of porphyrins.[8−10]

On the other hand, the antenna Chls of cyanobacteria, green plants, and FMO are not $\pi-\pi$-stacked. The nearest-neighbor Chls of these light-harvesting systems are asymmetrically

† Science University of Tokyo.
‡ Osaka University.
§ Nagoya University.
⊥ Tokyo Institute of Technology.

(1) Roszak, W.; Howard, T. D.; Southall, J.; Gardinar, A. T.; Law, C. J.; Isaaks, N. W.; Cogdell, R. J. *Science* **2003**, *302*, 1969–1972.
(2) (a) McDermott, G.; Prince, S. M.; Freer, A. A.; Hawthornthwaite-Lawless, A. M.; Papiz, M. Z.; Cogdell, R. J.; Isaacs, N. W. *Nature* **1995**, *374*, 517–521. (b) Koepke, J.; Hu, X.; Muenke, C.; Schulten, K.; Michel, H. *Structure* **1996**, *4*, 581–597.
(3) Boer, I.; Matysik, J.; Amakawa, M.; Yagai, S.; Tamiaki, H.; Holzwarth, A. R.; de Groot, H. J. M. *J. Am. Chem. Soc.* **2003**, *125*, 13374–13375.
(4) Amakawa, M.; Tamiaki, H. *Bioorg. Med. Chem.* **1999**, *7*, 1141–1144.
(5) (a) Liu, Z.-f.; Yan, H.-c.; Wang, K.; Kuang, T.-g.; Zhang, J.-p.; Gui, L.-l.; An, X.-m.; Chang, W.-r. *Nature* **2004**, *428*, 287–292. (b) Hino, T.; Kanamori, E.; Shen, J.-R.; Kouyama, T. *Acta Crystallogr.* **2004**, *D60*, 803–809.
(6) (a) Krauss, N.; Schubert, W. D.; Klukas, O.; Fromme, P.; Witt, H. T.; Saenger, W. *Nat. Struct. Biol.* **1996**, *3*, 965–973. (b) Ferreira, K. N.; Iverson, T. M.; Maghlaoul, K.; Barber, J.; Iwata, S. *Science* **2004**, *303*, 1831–1838. (c) Loll, B.; Kern, J.; Saenger, W.; Zouni, A.; Biesiadka, J. *Nature* **2005**, *438*, 1040–1044.
(7) (a) Fenna, R. E.; Matthews, B. W. *Nature* **1975**, *258*, 573–577. (b) Tronrud, D. E.; Schmidt, M. F.; Matthews, B. W. *J. Mol. Biol.* **1986**, *261*, 443–454.
(8) Takahashi, R.; Kobuke, Y. *J. Am. Chem. Soc.* **2003**, *125*, 2372–2373.
(9) Peng, X.; Aratani, N.; Takagi, A.; Matsumoto, T.; Kawai, T.; Hwang, I.-W.; Ahn, T. K.; Kim, D.; Osuka, A. *J. Am. Chem. Soc.* **2004**, *126*, 4468–4469.
(10) Hwang, I.-W.; Ko, D. M.; Ahn, T. K.; Yoon, Z. S.; Kim, D.; Peng, X.; Aratani, N.; Osuka, A. *J. Phys. Chem. B.* **2005**, *109*, 8643–8651.

aligned within the distance of 21 Å.[11] They probably obey the orientation rules that are different from those followed by LH1, LH2, and chlorosomes. Recent pump−probe experiments on CP43[12] and two-dimensional spectroscopy on FMO,[13] as well as theoretical studies on PS1[14] based on Förster's mechanism[15] and exciton theory,[16] showed that chlorophylls are ingeniously aligned in these light-harvesting systems, forming small clusters to collect and transfer the photon energy to the photosynthetic reaction center (RC).

How can we approach the antenna Chls of PS1, PS2, green plants, and FMO by porphyrin synthesis? Stimulated by the integration forms of Chls in LH1, LH2,[1,2] and RC[17]—they are analogous to *J*-aggregates[18] in stack structure—extensive studies on porphyrin arrays and aggregates have been conducted over the past decades[19] aiming at the development of model systems for LH1, LH2, and RC, as well as new electrooptical devices.[8,9,20,21] To synthesize porphyrin arrays and aggregates, three methods have thus far been proposed: (1) the direct binding of porphyrin skeletons via meso−meso linkage, coordination bonds,[8,9,22] and acetylene and olefin linkage,[23] (2) indirect alignments of porphyrins via covalent bonds, such as those represented by dendritic porphyrins,[24] peptide-linked porphyrins,[25] polymerized porphyrins,[26] metal-linked coordination bonds,[27] and (3) the aggregation of porphyrins through noncovalent interactions in solutions,[28] on the surface of solutions,[29] and in protein and proteinoid cavities.[30] Among the porphyrin arrays synthesized using these methods, those reported by Takahashi[8] and Peng[9] effectively mimic the ring-stacked and flat-ring morphologies, respectively, of the antenna Chls of LH1 and LH2.

(11) The 90 antenna Chls (Chl a) of cyanobacterial PS1 are distributed in three parallel ellipsoid rings so as to surround the reaction center (RC) maintaining the nearest-neighbor Mg−Mg distance within 7.6−21.0 Å (pdb 1jbo), whereas the 33 antenna Chls of PS2 are kept within 8.3−13.4 Å (pdb 1s5l) also surrounding the RC. The light-harvesting complexes, LHC-II, in the thylakoid membrane of chloroplasts exist as trimers, each of which comprises five Chl a and three Chl b on the stromal side, whereas there are three Chl a and three Chl b on the lumenal side. The antenna Chls on the stromal side form an ellipsoid ring (Mg−Mg; 9.8−12.8 Å); on the other hand those of the lumenal side form dimer (Mg−Mg; 9.3 Å) and tetramer (Mg−Mg; 8.2−12.5 Å) clusters (pdb 1rwt). The bacteriochlorophylls of FMO are distributed in a shallow funnel maintaining the Mg−Mg distance within 11.4−13.8 Å (pdb 4bcl).

(12) Di Donato, M.; van Grondelle, R.; van Stokkum, I. H. M.; Groot, M. L. *J. Phys. Chem. B* **2007**, *111*, 7345–7352.
(13) (a) Brixner, T.; Stenger, J.; Vaswani, H. M.; Cho, M.-H.; Blankenship, R. E.; Fleming, G. R. *Nature* **2005**, *434*, 625–628. (b) Engel, G. S.; Calhoun, T. R.; Read, E. L.; Ahn, T.-K.; Mančal1, T.; Cheng, Y.-C.; Blankenship, R. E.; Fleming, G. R. *Nature* **2007**, *446*, 782–786.
(14) Byrdin, M.; Jordan, P.; Kraus, N.; Fromme, P.; Stehlik, D.; Schlodder, E. *Biophys. J.* **2002**, *83*, 433–457.
(15) Förster, Th. *Discuss. Faraday Soc.* **1959**, *27*, 7–17.
(16) Rosenfeld, V. L. *Z. Phys* **1928**, *52*, 161. Bohm, D. *Quantum Theory*; Prentice-Hall: New York, 1961; p 427. Davydov, A. S. *Theory of Molecular Excitons*; McGraw-Hill: New York, 1962; pp 141−155. Davydov, A. S. *Theory of Molecular Excitons*; Plenum Press: New York, London, 1971; pp 23−112. Kasha, M.; Rawls, H. R.; El-Bayoumi, A. *Pure Appl. Chem.* **1965**, *11*, 371–392. Kasha, M. *Radiat. Res.* **1963**, *20*, 55–71.
(17) Deisenhofer, J.; Epp, O.; Miki, K.; Huber, R.; Michel, H. *Nature* **1985**, *318*, 618–624.
(18) (a) Jelley, E. E. *Nature (London)* **1936**, *138*, 1009. (b) Scheibe, G. *Angew. Chem.* **1936**, *49*, 563. (c) Fleisher, E. B.; Palmer, J. M.; Srivastava, T. S.; Chatterjee, A. *J. Am. Chem. Soc.* **1971**, *93*, 3162–3167. (d) Pasternack, R. F.; Huber, P. R.; Boyd, P.; Engasser, G.; Francesconi, L.; Gibbs, E.; Fasella, P.; Venturo, G. C.; Hinds, L. de C. *J. Am. Chem. Soc.* **1972**, *94*, 4511–4517. (e) Ohno, O.; Kaizu, Y.; Kobayashi, H. *J. Chem. Phys.* **1993**, *99*, 4128–4139.
(19) (a) Wasielewski, M. R. *J. Org. Chem.* **2006**, *71*, 5051–5066. (b) Wasielewski, M. R. *Chem. Rev.* **1992**, *92*, 435–461.
(20) (a) Aratani, N.; Osuka, A.; Kim, Y. H.; Jeong, D. H.; Kim, D. *Angew. Chem., Int. Ed.* **2000**, *39*, 1458–1462. (b) Nakano, A.; Yamazaki, T.; Nishimura, Y.; Akimoto, S.; Yamazaki, I.; Osuka, A. *Chem.—Eur. J.* **2000**, *6*, 3254–3271. (c) Tsuda, A.; Osuka, A. *Science* **2001**, *293*, 79–82.
(21) (a) Dalton, L. R.; Harper, A. W.; Ghosn, R.; Steier, W. H.; Ziari, M.; Fetterman, H.; Shi, Y.; Mustacich, R. V.; Jen, A. K.-Y.; Shea, K. *J. Chem. Mater* **1995**, *7*, 1060–1081. (b) Ogawa, K.; Ohashi, A.; Kobuke, Y. *J. Am. Chem. Soc.* **2003**, *125*, 13356–13357. (c) Collini, E.; Ferrante, C.; Bozio, R.; Lodib, A.; Ponterini, G. *J. Mater. Chem.* **2006**, *16*, 1573–1578.
(22) Morikawa, S.; Ikeda, C.; Kazuya Ogawa, K.; Kobuke, Y. *Lett. Org. Chem.* **2004**, *1*, 6–11.
(23) (a) Kelley, R. F.; Lee, S. J.; Wilson, T. M.; Nakamura, Y.; Tiede, D. M.; Osuka, A.; Hupp, J. T.; Wasielewski, M. R. *J. Am. Chem. Soc.* **2008**, *130*, 4277–4284. (b) Kelley, R. F.; Tauber, M. J.; Wilson, T. M.; Wasielewski, M. R. *Chem. Commun.* **2007**, 4407–4409. (c) Kelley, R. F.; Shin, W.-S.; Rybtchinski, B.; Wasielewski, M. R. *J. Am. Chem. Soc.* **2007**, *129*, 3173–3181. (d) Kelley, R. F.; Tauber, M. J.; Wasielewski, M. R. *Angew. Chem., Int. Ed.* **2006**, *45*, 7979–7982. (e) Song, H.-E.; Kirmaier, C.; Yu, L.; Bocian, D. F.; Lindsey, J. S.; Holten, D. *J. Phys. Chem. B* **2006**, *110*, 19121–19130. (f) Song, H.-E.; Kirmaier, C.; Yu, L.; Bocian, D. F.; Lindsey, J. S.; Holten, D. *J. Phys. Chem. B* **2006**, *110*, 19131–19139. (g) Hindin, E.; Forties, R. A.; Loewe, R. S.; Ambroise, A.; Kirmaier, C.; Bocian, D. F.; Lindsey, J. S.; Holten, D.; Knox, R. S. *J. Phys. Chem. B* **2004**, *108*, 12821–12832. (h) Rucareunu, S.; Mongin, O.; Schuwey, A.; Hoyler, N.; Gossauer, A. *J. Org. Chem.* **2001**, *66*, 4973–4988. (i) Vicente, M. G. H.; Jaquinod, L.; Smith, K. M. *Chem. Commun.* **1999**, 1771–1782. (j) Wytko, J.; Berl, V.; McLaughlin, M.; Tykwinski, R. R.; Schreiber, M.; Diederich, F.; Boudon, C.; Gisselbrecht, J.-P.; Gross, M. *Helv. Chim. Acta* **1998**, *81*, 1964–1977. (k) Yashnski, D. V.; Ponomarev, G. V. *Tetrahedron Lett.* **1995**, *36*, 8485–8488.
(24) (a) Choi, M.-S.; Aida, T.; Yamazaki, T.; Yamazaki, I. *Angew. Chem., Int. Ed.* **2001**, *40*, 3194–3198. (b) Yeow, E. K. L.; Ghiggino, K. P.; Reek, J. N.; Crossley, M. J.; Bosman, A. W.; Schenning, A. P. H. J.; Meujer, E. W. *J. Phy. Chem. B.* **2000**, *104*, 2596–2606.
(25) (a) Mihara, H.; Hareta, Y.; Sakamoto, S.; Nishino, N.; Aoyagi, H. *Chem. Lett.* **1997**, *54*, 731–737. (b) Tamiaki, H.; Onishi, M. *Tetrahedron: Asymmetry* **1999**, *10*, 1029–1032. (c) Solladié, H.; Hamel, A.; Gross, M. *Tetrahedron Lett.* **2000**, *41*, 6075–6078. (d) Fujitsuka, M.; Hara, M.; Tojo, S.; Okada, A.; Troiani, V.; Solladié, N.; Majima, T. *J. Phys. Chem. B,* **2005**, *109*, 33–35.
(26) (a) Takei, F.; Nakamura, S.; Onitsuka, K.; Ishida, A.; Tojo, S.; Majima, T.; Takahashi, S. *Chem. Lett.* **2003**, *32*, 506–507. (b) Takei, F.; Kodama, D.; Nakamura, S.; Onitsuka, K.; Takahashi, S. *J. Polym. Sci., Part A: Polym. Chem.* **2006**, *44*, 585–595. (c) Guildy, D. M.; Taieb, H.; Rahman, G. M. A.; Tagmatarchis, N.; Prato, M. *Adv. Mater.* **2005**, *17*, 871–875.
(27) (a) Kelley, R. F.; Goldsmith, R. H.; Wasielewski, M. R. *J. Am. Chem. Soc.* **2007**, *129*, 6384–6385. (b) Drain, C. M.; Hupp, J. T.; Suslick, K. S.; Wasielewski, M. R.; Chen, X. *J. Porphyrins Phthalocyanines* **2002**, *6*, 243–258. (c) Ikeda, A.; Ayabe, M.; Shinkai, S. *Chem. Lett.* **2001**, 1138–1139. (d) Richeter, S.; Jeandon, C.; Gisselbrecht, J.-P.; Ruppert, R.; Callot, H. J. *J. Am. Chem. Soc.* **2002**, *124*, 6168–6179. (e) Wilson, G. S.; Anderson, H. L. *Chem. Commun.* **1999**, 1539–1540. (f) Fan, J.; Whiteford, J. A.; Olenyuk, B.; Levin, M. D.; Stang, P. J.; Fleischer, E. B. *J. Am. Chem. Soc.* **1999**, *121*, 2741–2752.
(28) (a) Okamura, M. Y.; Feher, G.; Nelson, N. *Photosynthesis*; Govindjee, Ed.; Academic Press: New York, 1982; pp 195−272. (b) Pasternack, R. F.; Huber, P. R.; Boyd, P.; Engasser, G.; Francesconi, L.; Gibbs, E.; Fasella, P.; Venturo, G. C.; Hinds, L. D. *J. Am. Chem. Soc.* **1972**, *94*, 4511–4517. (c) Yamamura, T. *Chem. Lett.* **1977**, 773. (d) Yamamura, T. *Chem. Lett.* **1978**, 193. (e) Barber, D. C.; Freitag-Beeston, R. A.; Whitten, D. G. *J. Phys. Chem.* **1991**, *95*, 4074–4086. (f) Ribo, J. M.; Crusats, J.; Farrera, J.-A.; Valero, M. L. *J. Chem.Soc., Chem. Commun.* **1994**, 681–682. (g) Pasternack, R. F.; Schaefer, K. F.; Hambright, P. *Inorg. Chem.* **1994**, *33*, 2062–2065. (h) Akins, D. L.; Zhu, H.-R.; Guo, C. *J. Phys. Chem.* **1994**, *98*, 3612–3618. (i) Maiti, N.; Ravikanth, M.; Mazumdar, S.; Periasamy, N. *J. Phys. Chem.* **1995**, *99*, 17192–17197. (j) Akins, D. L.; Zhu, H.-R.; Guo, C. *J. Phys. Chem.* **1996**, *100*, 5420–5425. (k) Jin, R.-H.; Aoki, S.; Shima, K. *J. Chem. Soc., Faraday Trans.* **1997**, *93*, 3945–3953. (l) Bhyrappa, P.; Wilson, S. R.; Suslick, K. S. *J. Am. Chem. Soc.* **1997**, *119*, 8492–8502. (m) Maiti, N. C.; Mazumdar, S.; Periasamy, N. *J. Phys. Chem. B* **1998**, *102*, 1528–38. (n) Choi, M. Y.; Pollard, J. A.; Webb, M. A.; McHale, J. L. *J. Am. Chem. Soc.* **2003**, *125*, 810–820.
(29) (a) Xu, W.; Guo, H.; Akins, D. L. *J. Phys. Chem. B* **2001**, *105*, 1543–1546. (b) Okada, S.; Segawa, H. *J. Am. Chem. Soc.* **2003**, *125*, 2792–2796. (c) Sadasivan, S.; Köhler, K.; Sukhorukov, G. B. *Adv. Funct. Mater.* **2006**, *16*, 2083–2088.

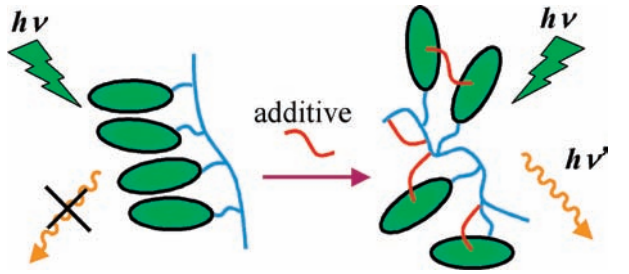

Figure 1. Schematic drawing of the *a posteriori* fluorescence optimization in porphyrin arrays.

In comparison with the antenna Chls in LH1, LH2, and chlorosomes, the asymmetric orientation of antenna Chls in cyanobacterial PS1, PS2, green plants, and FMO seems to be too complex to be mimicked by porphyrin synthesis. It is clear that the deterministic approach such as those[8,9] adopted for the $\pi-\pi$ stacked Chl systems of LH1 and LH2 is not applicable. The asymmetry may be achieved through cross-linkage such as adopted by Crossley[31] and Pandy[32] for the synthesis of dimer porphyrins; however, the synthesis will require a tremendous amount of work for the arrays or clusters larger than dimer and for the arrays optimized in fluorescence emission.

A simple means involves (1) the reduction in dimensionality from 2 or 3 to 1, that is, to use oligomeric or polymeric porphyrins conserving the distance among neighboring porphyrins within 6−20 Å (like that in naturally occurring antenna Chls) and (2) the construction of a tunable system that is responsive to additives in fluorescence emission. Such systems allow the *a posteriori* optimization of fluorescence emission and dye orientation. For this purpose, peptide-linked porphyrin arrays in which compact porphyrins are bound to the peptide chains via a "short linker" are suitable. Porphyrins in such an array are proximally constrained and maintain their mutual orientation through the balance of the van der Waals interaction ($\pi-\pi$ interaction), ligand coordination, and peptide folding. The addition of a ligand that coordinates to the central atoms of porphyrins or interacts with the amide moiety of the peptide chain by hydrogen bonds would break this balance to force porphyrins to form a new conformation (Figure 1). By searching for such ligands, we expect to find an optimal additive for efficient fluorescence emission, which is an index of the suppression of the thermal quenching of absorbed photon energies.

The porphyrin arrays used in this study are Boc−$(Por^{M,S})_n$−OBu^t (M = H2 and Zn; n = 2, 4, and 8; Figure 2; details of the synthesis, see Supporting Information1) elongated from the protected unnatural amino acid Boc−$Por^{H2,S}$−OBu^t (**4**; Scheme 1)[33] that were synthesized by connecting the β-pyrrole position of 5,10,15,20-tetra-*n*-butyl porphyrin (H_2TBP)

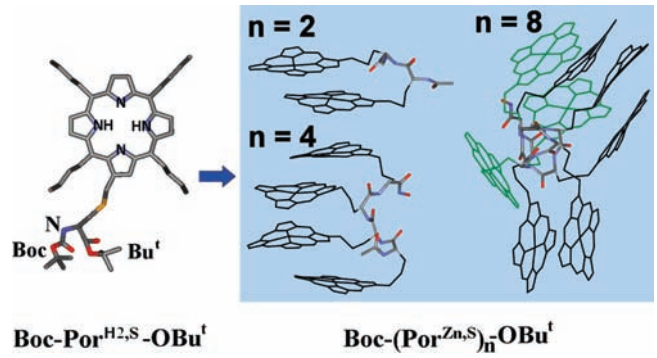

Figure 2. Protected metal-free monomer Boc−$(Por^{H2,S})$−OBu^t, **4**, and its zinc oligomers Boc−$(Por^{Zn,S})_n$−OBu^t (n = 2, 4, and 8): dimer Boc−$(Por^{Zn,S})_2$−OBu^t, **6′**; tetramer Boc−$(Por^{Zn,S})_4$−OBu^t, **7′**; and octamer Boc−$(Por^{Zn,S})_8$−OBu^t, **8′**. The lowest-energy structures of **6′**, **7′**, and **8′** calculated by AMBER6.0. are shown here.

Scheme 1. [1] Synthetic Route for Boc−$(Por^{M,S})_n$−OBu^t (M = H_2 and Zn; n = 1, 2, 4, and 8)[a]

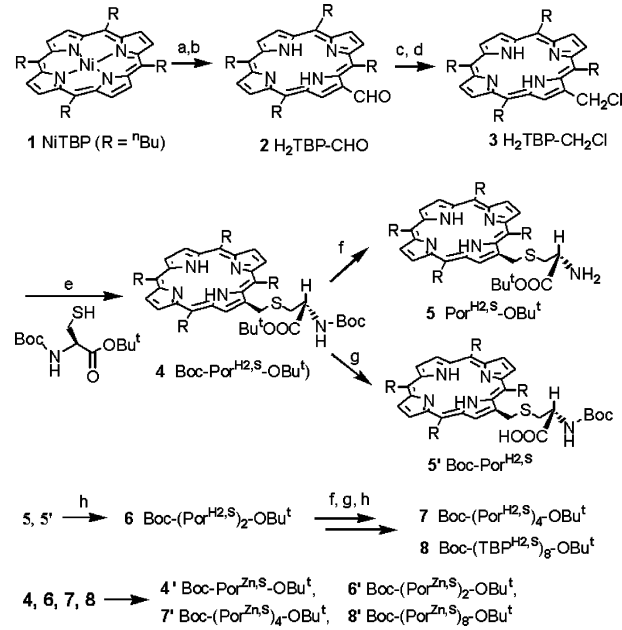

[a] Reagents and conditions: (a) DMF, $POCl_3$, 1,2-dichloroethane, reflux, 2.5 h, followed by NaOAc, 60%; (b) conc. H_2SO_4, silica gel column ($CHCl_3$), 30%; (c) $NaBH_4$, THF, 45°C, 15 min, 85%; (d) $SOCl_2$, pyridine, CH_2Cl_2, −78°C, 95%; (e) THF, Ar, rt, 1 h, 78%; (f) TFA, thioanisole, CH_2Cl_2, 0°C → rt, 1 h, 90%; (g) TFA, thioanisole, CH_2Cl_2, rt, 15 h; $(Boc)_2O$, DIEA, rt, 2 h, 92%; (h) PyBOP, DIEA, DMF, 0°C → rt, 2 h, 88%.

with the C_α of cysteine via a C−S−C_β linker. This short linker helps in maintaining the nearest-neighbor porphyrins in the arrays within 6−20 Å in Zn−Zn distance—close to the Mg−Mg distance of Chls in PS1 and others. In comparison with the known peptide-type arrays that have bulky porphyrins attached to them via long side chains of Lys, Orn, and Glu,[25] our arrays are characteristic of the compactness of the used porphyrin, as well as the shortness of the linker part (C−S−C_β). However, the linker is not too short to hinder the rotations of porphyrins, but it is moderately short to allow the arrays to flexibly respond to additives.

A search for additives that optimize the fluorescence of oligomers revealed the superiority of 1,2- diaminoethane (en). Sufficient amounts of en increased the fluorescence integrated intensities of the dimer, tetramer, and octamer by ∼12, ∼12,

(30) (a) Rabanal, F.; DeGrado, W. F.; Dutton, P. L. *J. Am. Chem. Soc.* **1996**, *118*, 473–474. (b) Nango, M.; Kashiwada, A.; Watanabe, H.; Yamada, S.; Yamada, T.; Ogawa, M.; Tanaka, T.; Iida, K. *Chem. Lett.* **2002**, 312–313. (c) Endo, M.; Fujitsuka, M.; Majima, T. *Chem.−Eur. J.* **2007**, *13*, 8660–8666.

(31) Crossley, M. J.; Hambley, T. W.; Mackay, L. G.; Try, A. C.; Walton, R. *J. Chem. Soc., Chem. Commun.* **1995**, 1077–1072. Crossley, M. J.; Mackay, L. G.; Try, A. C. *J. Chem. Soc., Chem. Commun.* **1995**, 1925–1927.

(32) Zheng, G.; Shibata, M.; Dougherty, T. J.; Pandey, R. K. *J. Org. Chem.* **2000**, *65*, 543–557.

(33) Abbreviations: Boc, *tert*-butoxycarbonyl; DIEA, diispropylethylamine; OBu^t, *tert*-butyl ester; PyBOP, benzotriazole-1-yl-oxy-tris-pyrroridino-phosphonium hexafluorophosphate; TFA, trifluoroacetic acid.

and >730 times—excited at 564 nm—, respectively, when compared with those observed in the absence of en.

Our results demonstrate the potentiality of the tunable dye polymers that are *a posteriori* optimized in fluorescence emission by additive reagents for the development of effective light-harvesting materials.

2. Results and Discussion

2.1. Porphyrin Interactions in the Arrays. The results of the ^{1}H NMR experiments suggest that porphyrins in Boc−(Por^{Zn,S})$_2$−OBu^t (**6′**) are in a face-to-face-like interaction. The signals of **6′** in the ring-proton region showed a large high-field shift from 9.2−9.4 ppm of the monomer and spread over 7.82−9.08 ppm accompanying a strong line broadening (Supporting Information 2). This result indicates that the β-pyrrole protons of **6′** are under the influence of mutual ring currents. Because of this broadening, NOESY experiments were impossible in the temperature range from −50 to +50 °C.[34]

On the other hand, the B-band regions of the AB spectra of **6′**, Boc−(Por^{Zn,S})$_4$−OBu^t (**7′**), and Boc−(Por^{Zn,S})$_8$−OBu^t (**8′**) show blue shifts (about 14 nm from 424 nm of ZnTBP) and band splittings (Supporting Information 3). This result indicates that the porphyrins of these oligomers assume weakly skidded face-to-face orientations in the arrays, corresponding to the result of the NMR measurement mentioned above. The B-bands obey Beer's law in organic solvents such as CH_2Cl_2 and benzene (<10^{-4} M) in appearance, suggesting that the blue shift originates from an intramolecular porphyrin interaction. The deconvolution of the B band regions of **6′**, **7′**, and **8′** indicate that their spectra are composed of four common peaks: peak 1 (410 nm, predominant), peak 2 (422−427 nm, shoulder), peak 3 (389 nm), and peak 4 (434 nm) (Supporting Information 4). The last two peaks appear at the lower- and higher-energy tails of the predominant peaks of the tetramer and octamer. The relative ratio of peak 2 decreases with increasing n; however, those of peaks 3 and 4 increase with the line width broadening.[35]

6′ shows a weak positive exciton chirality (Supporting Information 3), whereas **7′** shows a negative exciton chirality larger than that of **6′**, giving peaks at 412 (48.1 cm^2·mmol^{-1}) and 427 nm (−67.6 cm^2·mmol^{-1}), which correspond to the first and second peaks, respectively, of the AB spectrum of this compound.[36] The CD spectrum of **8′** has two types of CD peaks that differ in line width and concentration dependence: a sharp and negative one at 390 nm and a broad one showing positive and negative peaks at 399 and 429 nm, respectively, with the zero-cross point at 413 nm. The peak at 390 nm is concentration dependent in the concentration range from 10^{-8} to 10^{-4} M and particularly increases in the concentration range from 10^{-5} to 10^{-4} M with a decrease in the intensities of the 399 and 429 nm peaks.[37] Consequently, all porphyrins in these arrays are asymmetrically arranged to each other.

Table 1. Results of Fluorescent Search[a]

ligand	Q-band shift (nm)	fluorescence shift (nm)	Φ'[b]
en	13, 17	25	0.078
pn	15, 17	13	0.041
im	15, 18	13	0.034
bn	−	3	0.021
dabco	−	0	0.014
hmta	−	9	0.013

[a] Porphyrins were excited at 564 nm in CH_2Cl_2. Data were collected at sufficiently diluted concentration (~2 × 10^{-6} M) using a cell with a optical path length of 5 mm to avoid self-absorption. [b] Corrected for the fluorescence yield of ZnTPP or the monomer Boc−Por^{Zn,S}−OMe.

2.2. Fluorescence Behavior of Boc−(Por^{Zn,S})$_n$−OBu^t. The porphyrin interaction predominated by a face-to-face-like orientation is not advantageous for efficient fluorescence emission because of photon energy quenching through the thermal processes. In practice, the apparent fluorescence yield of Boc−(Por^{Zn,S})$_n$−OBu^t decreases with increasing n, obeying $\Phi' = 0.03/n^{1.5}$ (Supporting Information 5). Therefore, we searched for the additives that enhance fluorescence emission.

2.3. Fluorescence Control of 6′. Considering the results of the AB experiments on **7′** and **8′**, which suggest the mixing of pairwise face-to-face-like interactions of porphyrins similar to that of **6′**, we subjected **6′** to the fluorescence condition search. In this search, we compared the effect of monodentate, bidentate, and multidentate ligands to control the porphyrin orientation: 1,3-diazacyclopenta-2,4-diene (im; imidazole), en, 1,3-diaminopropane (pn), 1,4-diaminobutame (bn), 1,4-diazabicyclo[2.2.2]octane (dabco), and 1,3,5,7-tetraazatricyclo[3.3.1.1^{3,7}]decane (hmta; hexamethylenetetramine). The results of this search are listed in Table 1. Evidently, en is superior to the other ligands in terms of fluorescence recovery. The table seems to indicate that (1) the bulkier the ligand, the smaller the fluorescence recovery and (2) the lower the coordination ability of the ligand, the weaker the fluorescence recovery. Figure 3 demonstrates that en induces marked fluorescence intensity and line shape, as well as absorption, changes in **6′**. Although ligands other than en cause line shape changes in the fluorescence spectra, they are not as efficient as en in fluorescence recovery (Supporting Information 6). Molecular modeling showed that en is sufficiently small to penetrate into the interstitial spaces of the arrays and to interact with hidden Zn^{2+} ions, amide moieties, and sulfur atoms.

As shown in Figure 3, the Q-band absorption peaks at 564 and 602 nm of **6′** asymptotically approach 577 and 620 nm, respectively, with the addition of en. The titration curves observed at 564 and 620 nm indicate that it requires more than ~**5** equiv of en to complete the spectral change. The addition

(34) Boc−(Por^{H2,S})$_2$−OBu^t showed more than 18 lines of a complicated mixture of singlets, doublets, quartets, and multiplets spread over 0.7 ppm in the β-pyrrole region. The signals showed high-field shifts as compared to those of the monomer Boc−Por^{H2,S}−OBu^t. Unfortunately, we could not assign the off-diagonal peaks arising from the porphyrin−porphyrin interaction in **6′** in the NOESY spectrum. However, note that the NMR chart of Boc−(Por^{H2,S})$_2$−OBu^t showed the existence of a water molecule that interacts with the pyrrole NH. Further addition of water had no effect on the visible AB, CD, or NMR spectra.

(35) The metal-free base monomer Boc−Por^{H2,S}−OBu^t exhibits a B-band peak at 412 nm. This peak splits into two showing a new shoulder on the higher-energy side (405−406 nm) in organic solvents such as $CHCl_3$, CH_2Cl_2, and C_6H_6, indicating that the number of face-to-face stacks of porphyrins increases in the arrays with n. The porphyrin interactions in the free-base oligomers **6**, **7**, and **8** are weak when compared with those in the Zn compounds **6′**, **7′**, and **8′**. The deconvolution of the B bands of **6**, **7**, and **8** showed that the bands are also composed of four common bands similar to those of the Zn compounds.

(36) The molar ellipticities of metal-free bases (**6**, **7**, and **8**) were much different from those of the zinc compounds **6′**, **7′**, and **8′**.

(37) The intensity of the peak at 390 nm, as well as the peaks at 399 and 429 nm, is proportional to the logarithm of the concentration, probably indicative of the consecutive aggregation of the octamer. Considering the small occupancy of the peak at 390 nm in the AB spectrum, the estimated molar ellipticity [θ] reached up to ~108 mdeg·cm^2·mol^{-1}. The molar ellipticity, strong blue shift, and sharp linewidth of the species giving the peak at 390 nm suggest that the species originates from H-like aggregation. MD calculations suggest that the main chain of **8′** assumes a pleated helix structure. The strong CD of the peak at 390 nm may originate from the formation of an intermolecular double-stranded β-sheet, where the porphyrins are aligned with a face-to-face (and $\pi-\pi$-stacked) conformation.

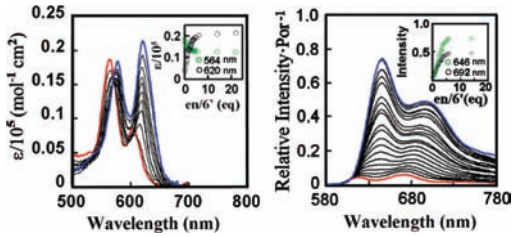

Figure 3. Results of titration for Boc−(Por^{Zn,S})$_2$−OMe, **6′**, in CH_2Cl_2 (2.24×10^{-6} M) with 1,2-diaminoethane (en, 0−20 equiv). All the spectra were observed in an Ar atmosphere. Cells with optical path lengths of 1.0 mm, 5 mm, and 10 mm were used for the absorption experiments; on the other hand a cell with an optical path length of 5 mm was used for fluorescence experiments. The absorption change in the Q-band region (left: per molecule) and the fluorescence change (right: per porphyrin, corrected for self-absorption, excited at 564 nm) are presented. The spectra are shown in a thinned-out form for clarity. Spectra shown by the thick solid red lines are those observed in the absence of en. Spectra shown by the thick solid blue lines are those observed in the presence of an excess amount (22 equiv) of en. The insets show the titration curves observed by the absorption and fluorescence methods.

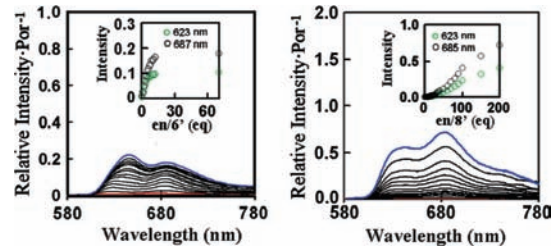

Figure 4. Results of titration for Boc−(Por^{Zn,S})$_4$−OMe (left) and Boc−(Por^{Zn,S})$_8$−OMe (right) in CH_2Cl_2 (2.00×10^{-6} M) with en followed by fluorescence spectroscopy. A cell with a 5-mm optical path length was used. The spectra corrected for self-absorption are shown in a thinned-out form for clarity. All the spectra were observed in an Ar atmosphere. The spectra shown in red are those observed in the absence of en. The spectra shown in blue are those observed in the presence of 70 and 200 equiv of en for **7′** and **8′**, respectively.

of an excess amount of en to **6′** enhances the fluorescence intensity to a level about 12 times larger than that observed in the absence of en in integrated (580−800 nm) intensity. Considering the fact that en also increases more than 4−5 times[38] the fluorescence intensity of the monomer (Boc−Por^{Zn,S}−OBu^t, **4′**) (Supporting Information 7), the recovery ratio per porphyrin reaches up to 63% of the monomer level. When it is compared with that of **4′** itself, the value reaches 370% of the monomer. Further, en causes marked changes in fluorescence line shape. The fluorescence peaks of **6′** at 617 and 672 nm asymptotically approach 646 and 692 nm, respectively, during en titration. The titration curves at 646 and 692 nm also indicate that more than 5 equiv of en is necessary to complete change of the spectrum of **6′**. Note that any of these fluorescence maxima differ from those of **4′** (609 and 660 nm in the absence of en and 640 and 686 nm in the presence of an excess amount of en).

2.4. Fluorescence Recovery in Tetramer and Octamer. Encouraged by the success in investigating **6′**, we studied the effects of en on **7′** and **8′**. Here, en also caused marked changes in fluorescence line shape and intensity. The results corrected for self-absorption at excitation and emission wavelengths are shown in Figure 4. The fluorescence peaks of **7′**, observed at 623 and 678 nm in the absence of en, asymptotically approach 647 and 687 nm, respectively, and the fluorescence titration curve observed at 623 nm indicates that more than ∼12 equiv of en are necessary for sufficient increase of the fluorescence. The fluorescence peaks of **8′** at 636 and 667 nm, observed in the absence of en, asymptotically approach 643 and 685 nm, respectively. However, the titration feature is apparently different from those of **6′** and **7′**. The fluorescence titration curves observed at 623 and 685 nm are neither asymptotic nor monotonic[39] and indicate that more than 200 equiv of en is necessary to relax the porphyrin−porphyrin interaction. The line shapes of **7′** and **8′** in the absence or presence of en indicate that these oligomers differ in exciton interactions and electronic relaxation. In any event, the addition of a sufficient amount of en increases the fluorescence of the tetramer and octamer by ∼12 and >760 times, respectively, when compared with that observed in the absence of en. The recovery ratio per porphyrin reaches up to the 20 and 67% of **4′**/en for **7′** and **8′**, respectively, in integrated intensities. In comparison with the fluorescence of **4′** itself, the values reach up to 87 and 287% of the monomer.

2.5. Fluorescence Lifetime. The fluorescence lifetimes of the arrays are short in the absence of en (Figure 5) concurrent with the decrease in the fluorescence yield (Φ′) (Supporting Information 5). The fluorescence of ZnTBP obeys single-lifetime (1.58 ns) decay, whereas those of **6′**, **7′**, and **8′** obey two- lifetime decay, namely, short ($\tau_s = 0.49$, 0.54, and 0.55 ns, respectively) and long (τ_l = 1.58. 1.48, and 1.46 ns, respectively). The contribution of long-lifetime decay decreases with the array size (Figure 5, upper four plots). This result is consistent with the estimation that Zn porphyrins in **7′** and **8′** are face-to-face-like paired similarly to those in **6′** (see the section of Porphyrin Interactions in the Arrays). The short lifetime may correspond to the paired porphyrins, whereas the long lifetime may arise from the unpaired porphyrins that are generated at the termini of peptide chains during array fluctuations. On the other hand, in the presence of sufficient amounts of en (22.0 equiv for **6′**, 70 equiv for **7′**, and 200 equiv for **8′**), the lifetimes of the arrays (τ = 2.24, 2.04, and 1.98 ns for **6′**, **7′**, and **8′**, respectively) are close to that of ZnTBP (τ = 2.10 ns). This means that en decreases the face-to-face-like pairwise interactions among porphyrins in the arrays (Figure 5, lower four plots). Note that en also elongates the lifetime of ZnTBP itself from 1.58 to 2.10 ns through coordination.

2.6. Asymptotic Changes of the AB and CD Spectra of 6′, 7′, and 8′. To study the conformation changes of **6′**, **7′**, and **8′** through exciton chirality before and after en addition, we monitored the AB and CD spectra of the B-band region. The

(38) The absorption change of Boc−Por^{Zn,S}−OBu^t (**4′**) in CH_2Cl_2 (2.08×10^{-6} M) upon addition of 1,2-diaminoethane (en) was simulated by assuming the simple association equilibrium A + B ⇆ AB, where A = **4′**, B = en, and AB = **4′**·en. This afforded an association constant K = 28100 mol^{-1} (see Figure S-8b in Supporting Information). However, the gradual increase of the fluorescence of **4′** observed at 641 nm—it increases up to ∼5 times—upon addition of en (see the inset of Figure S-7a in Supporting Information) and that observed at 609 nm are not accounted for by the simple association equilibrium adopted for the simulation of the absorption change.

(39) The spectra are corrected for the absorption at excitation and emission wavelengths. The absorption of **8′** at the excitation wavelength (564 nm) increases with increasing the amounts of en, whereas those of **6′** and **7′** decrease at 564 nm; therefore, the feature of fluorescence increase of **8′** is expected to be larger than those of **6′** and **7′** because of this correction. The reason for the abnormal increase of **8′**, particularly the increase in the region of en >100 equiv, is not clear. The addition of excess amounts of en might cause a local change of the media around the molecule considering the results together with those of the fluorescence changes of **4′**.

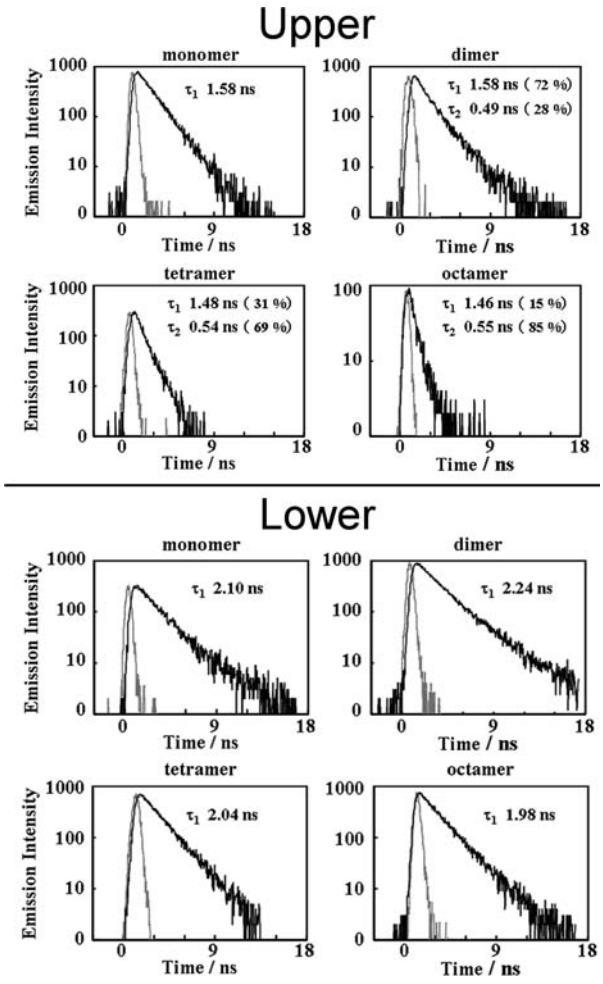

Figure 5. Results of fluorescence lifetime measurements for monomer (**4′**), dimer (**6′**), tetramer (**7′**), and octamer (**8′**). The upper four plots are those measured at 640 nm in the absence of en; the lower four plots are those measured at 660 nm in the presence of sufficient amounts of en (22.0 equiv for **6′**, 70 equiv for **7′**, and 200 equiv for **8′**).

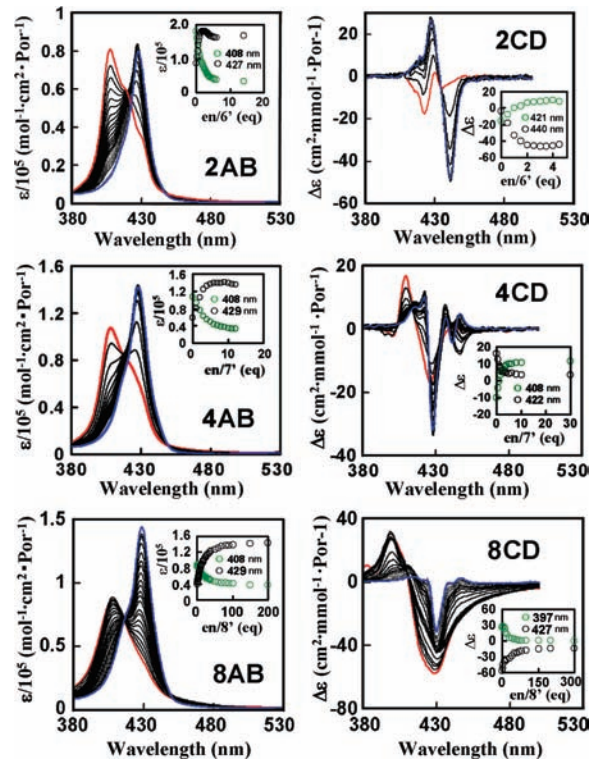

Figure 6. B-band regions of the visible AB (left) and CD (right) spectra of Boc−$(Por^{Zn,S})_2$−OMe (2.00×10^{-6} M, upper), Boc−$(Por^{Zn,S})_4$−OMe (2.00×10^{-6} M, middle), and Boc−$(Por^{Zn,S})_8$−OMe (1.97×10^{-6} M, lower) in CH_2Cl_2 upon the addition of en. Cells with an optical path length of 10 mm were used for AB and CD experiments. All of the spectra were observed in an Ar atmosphere. Insets show the titration curves. Spectra shown in red are those observed in the absence of en. Spectra shown in blue are those observed in the presence of excess amounts of en (22.0 equiv for **6′**, 70 equiv for **7′**, and 200 equiv for **8′**). All of the spectra are corrected for those per porphyrin.

results are shown in Figure 6. The figure clearly shows that the porphyrins in the arrays do not lose exciton chirality even in the presence of sufficient amounts of en and that the porphyrin of the oligomers asymptotically approach new orientations. The AB spectrum observed in the presence of a sufficient amount of en is similar to the B-band spectrum of the monomeric pentacoordinate ZnTBP (λ_{max} = 427 nm). The absorption intensity of **6′** at 408 nm decreases with the addition of en, whereas that at 427 nm increases. The titration curve of the latter indicates that **6′** binds two or three en molecules at first, which markedly changes the absorption, then binds additional two or three en. Several isosbestic points were observed in the expanded spectra (Supporting Information 8). The spectra shifted stepwise with the addition of en showing three or four cross points, which indicates that consecutive multistep interactions occur between porphyrins and en in the mixture. This result is in agreement with that of the ^{1}H NMR experiments observed in $CDCl_3$ (Supporting Information 2), where the broad and high-field-shifted spectrum of **6′** without en returns, in the presence of en, to the original low field of the monomeric porphyrin showing signal narrowing. However, it approaches a new spectrum composed of approximately nine signals, which differs from the monomer spectrum composed of only three signals (1H at 9.534 ppm, 4H at 9.446 ppm, and 2H at 9.409 ppm). These results indicate the following: (1) at least two en molecules interact with **6′**; (2) each porphyrin is under the influence of the ring current of the partner porphyrin in the absence or presence of en, but the effect of ring current is slight in the latter; and (3) the mutual positions of the two porphyrins in the new structure is fixed. Consequently, in conjunction with the results of the visible AB experiments, it is probable that two en molecules coordinate with Zn^{2+} at the first stage, which makes each porphyrin almost independent of the influence of the ring current of its partner; then, the third en may interact with the amide moiety of the main chain. However, the porphyrins are still sufficiently within the range of exciton interactions. Unfortunately, it is impossible to obtain the NOESY or ROESY spectrum that is useful for the structural analysis of **6′**/en.

Irrespective of the absence or presence of en, it was impossible to deconvolute the CD spectra of **6′** using ideal positive and negative pairs of Cotton-effect that exhibit zero-cross points at the absorption maxima.[40] This suggests that several energy bands that differ in wavelength, intensity, and line width contribute to the AB and CD spectra. The CD spectrum of **6′** in the presence of a sufficient amount of en shows the contribution of two components: a small one observed in the short-wavelength region and a large one observed in the

(40) Yamamura, T.; Mori, T.; Tsuda, Y.; Taguchi, T.; Josha, N. *J. Phy. Chem., A* **2007**, *111*, 2128–2138.

long-wavelength region. Both components show the negative first and positive second Cotton effects that are characteristic of negative chirality. The zero-cross point (432 nm) of the large component is close to the absorption maximum (427 nm).

Tetramer **7′** and octamer **8′** also show asymptotic changes in the AB and CD spectra of the B-band region (Figure 6). The addition of en to **7′** decreases the absorption intensity at 408 nm and increases that of the new peak at 429 nm. The titration curves of **7′** observed at 408 and 429 nm (shown in the inset) indicate that more than 10 equiv of en is necessary for **7′** to relax its $\pi-\pi$ interaction. The addition of en to **8′** also decreases the intensity of the absorption peak at 408 nm, simultaneously increasing the intensity of the new peak at 429 nm. The titration curves at 408 and 429 nm (shown in the inset) indicate that more than 100 equiv of en is necessary for **8′** to relax its $\pi-\pi$ interaction.

As mentioned above, our tunable porphyrin arrays asymptotically approach new CD-active structures. The morphological analogy of the asymmetric orientation of an antenna model can be discussed by the R, Θ, Φ, ϕ, θ, and Ψ of the nearest-neighbor dyes, where R, Θ, and Φ denote the polar coordinates between the central atoms of adjacent dyes; on the other hand, ϕ, θ, Ψ denote the Euler angles between the planes of the adjacent dyes (Supporting Information 9), because an orientation analysis of the nearest-neighbor Chls in cyanobacterial PS1, PS2, green plants, and FMO shows that they distribute in specific areas of (R, Θ, Φ, ϕ, θ, Ψ) (Supporting Information 10). Search of the synthetic models—irrespective of polymer types, such as those we provided here, or cross-linked types—that show an analogy in the distribution of (R, Θ, Φ, ϕ, θ, Ψ) among the nearest-neighbor dyes, as well as efficient fluorescence yields, may lead to the development of new antenna models for any of PS1, PS2, green plants, and FMO.

2.7. Concluding Remarks. (1) Peptide-linked porphyrins Boc−$(Por^{Zn,S})_n$−OBu^t (n = 2, 4, and 8) were synthesized. The oligomers showed a blue shift in the B-band regions of the absorption spectra and a decrease in the fluorescence intensity with increasing n, as well as circular dichroism. The fluorescence was markedly recovered by the addition of 1,2-diaminoethane (en). (2) We succeeded in demonstrating the potentiality of the dye oligomers responsive to additive reagents as light-harvesting materials. Tunable dye polymers may be potential for the modeling of the antenna chlorophylls observed in nature.

3. Experimental Section

3.1. Synthetic Route. The synthesis of Boc−$(Por^{M,S})_n$−OBu^t (M = H_2 and Zn; n = 1, 2, 4, and 8) was performed according the route shown in Scheme 1. All the reactions were carried out in an Ar atmosphere. The reactions involving porphyrinic amino acids were conducted in the dark. The synthesis of porphyrinic amino acids started from 5,10,15,20-tetra(*n*-butyl)porphyrin, H_2TBP (**1**),[41] which was prepared from pyrrole and diethoxypentane[42] using the method of Lindsey et al.[43] H_2TBP was converted to 5,10,15,20-tetra(*n*-butyl)porphyrin-2-carbaldehyde, H_2TBP-CHO (**2**), by passing through [5,10,15,20-tetra(*n*-butyl) porphyrinato(2-)]nickel(II)-2-carbaldehyde, NiTBP-CHO, which was prepared from [5,10,15,20-tetra(*n*-butyl)porphyrinato(2-)]nickel(II) employing the Vilsmeier reaction.[44] The demetalation of NiTBP-CHO to **2** was carried out using conc. H_2SO_4.[45] **2** was reduced by $NaBH_4$ in THF to 2-hydroxymethyl-5,10,15,20-tetra(*n*-butyl)porphyrin, H_2TBP-CH_2-OH, from which 2-chloromethyl-5,10,15,20-tetra(*n*-butyl)porphyrin, H_2TBP-CH_2Cl (**3**), was derived by treatment with $SOCl_2/CH_2Cl_2$ in the presence of pyridine. The chloromethyl group of **3** was so labile that **3** was not purified on silica gel columns. It should only be washed quickly with water and dried in vacuo and then used for coupling with Boc−Cys(SNa)−OBu^t, which was prepared from Boc−Cys(SH)−OBu^t and NaH in THF. Boc−Cys(SH)−OBu^t was prepared by reducing Boc−cystine−OBu^t with dithiothreitol in $CHCl_3$. Boc−cystine−OBu^t was derived from commercial cystine−OBu^t by the reaction with Boc_2O in dioxane/water. The coupling of Boc−Cys(SNa)−OBu^t with **3** afforded 2-*tert*-butoxycarbonylamino-3-[5,10,15,20-tetra(*n*-butyl)porphyrin]-2-yl-methylsulfanyl-propionic acid *tert*-butyl ester, Boc−$Por^{H2,S}$−OBu^t (**4**). The elongation of this monomer to the dimer Boc−$(Por^{H2,S})_2$−OBu^t (**6**) was carried out by coupling $Por^{H2,S}$−OBu^t (**5**) with Boc−$Por^{H2,S}$ (**5′**) in DMF using PyBOP and DIEA as coupling reagents. The oligomers Boc−$(Por^{H2,S})_4$−OBu^t (**7**), and Boc−$(Por^{H2,S})_8$−OBu^t (**8**) were similarly prepared from the corresponding precursors. Finally, their Zn correspondents Boc−$(Por^{Zn,S})_2$−OBu^t (**6′**), Boc−$(Por^{Zn,S})_4$−OBut (7′), and Boc−$(Por^{Zn,S})_8$−OBu^t (**8′**) were respectively derived from **6**, **7**, and **8** by reacting them with $Zn(CH_3COO)_2 \cdot 2H_2O$ in $CHCl_3$. Details of the synthesis are given in Supporting Information 1.

3.2. Physicochemical Measurements. Reagents for physicochemical measurements were purchased from Sigma-Aldrich Corp. UV−visible absorption (AB) spectra were recorded on a Shimadzu UV2450 spectrophotometer using quartz cells with optical path lengths of 0.01, 0.1, and 1 cm at room temperature in an Ar atmosphere. The CD spectra were recorded on a JASCO J-725 spectropolarimeter using a quartz cell with an optical path length of 0.1 cm in an Ar atmosphere. They were averaged for three or five measurements and then smoothed. Fluorescence spectra were recorded on a Shimadzu RF-5300PC fluorescence spectrometer using a quartz cell with a optical path length of 0.5 cm at room temperature in an Ar atmosphere and were corrected on 4-dimethylamino-4-nitrostilben, 4-aminophtalimide, and quinine sulfate. The fluorescence lifetime was measured at 645 and 660 nm in the absence and presence of en, respectively, using a Hamamatsu Photonics Picosecond Fluorescence Lifetime Measurement System C4780 (composed of the dye laser LN203S2 with 2-(4-biphenyl)-6-phenylbenzoxazole (peak wavelength: 400 nm), the streak scope C4334-02, and the triggering unit C4792) with a time range of 20 ns.

Acknowledgment. We thank Professor Masa-aki Haga of Chuo University for assisting in the mass spectral measurement and Professor Makoto Onaka of The University of Tokyo for the discussions on meso-alkyl porphyrin synthesis. This work was supported by a Grant-in-Aid for Scientific Research on Priority Areas (417) from the Ministry of Education, Culture, Sports, Science and Technology (MEXT) of the Japanese Government.

(41) (a) Jentzen, W.; Simpson, M. C.; Hobbs, J. D.; Song, X.; Ema, T.; Nelson, N. N. Y.; Medforth, C. J.; Smith, K. M.; Veyrat, M.; Mazzanti, M.; Ramasseul, R.; Marchon, J.-C.; Takeuchi, T.; Goddard, W. A.; Shelnutt, J. A. *J. Am. Chem. Soc.* **1995**, *117*, 11085–11097. (b) Senge, M. O.; Bischoff, I.; Nelson, N. Y.; Smith, K. M. *J. Porphyrins Phthalocyanines* **1999**, *3*, 99–116.

(42) 1,1-Diethoxypentane was synthesized by treating *n*-valeraldehyde (100 g, 0.89 mol) with $CaCl_2$ (20.6 g, 1.86×10^{-1} mol) in ethanol for 2 h. The organic layer was washed with water three times, dried on K_2CO_3 and $LiAlH_4$, and finally distilled under reduced pressure. The yield was 143.2 g (77%).

(43) (a) Lindsey, J. S.; Schreiman, I. C.; Hsu, H. C.; Kearney, P. C.; Marguerettaz, A. M. *J. Org. Chem.* **1987**, *52*, 827–836. (b) Li, F.; Yang, K.; Tyhonas, J. S.; MacCrum, K. A.; Lindsey, J. S. *Tetrahedron* **1997**, *53*, 12339–12360. (c) Gonsalves, A. M. d'A. R.; Pereira, M. M. *J. Heterocycl. Chem.* **1985**, *22*, 931–933.

(44) (a) Vilsmeier, A.; Haack, A. *Chem. Ber.* **1927**, *60*, 119–122. (b) Ponomarev, G. V.; Maravin, G. B. *Chem. Heterocycl. Compd.* **1982**, *18*, 50–55. (c) Callot, H. J. *Tetrahedron* **1973**, *29*, 899–901.

(45) (a) Yeh, Chen-Y.; Miller, S. E.; Carpenter, S. D.; Nocera, D. G. *Inorg. Chem.* **2001**, *40*, 3643–3646. (b) Lavallee, D. K. *Coord. Chem. Rev.* **1985**, *61*, 55–96.

Supporting Information Available: Synthesis of the porphyrin arrays, ^{1}H NMR spectral change of Boc−(Por^{Zn,S})$_2$−OBu^t, Soret band regions of absorption and circular dichroism spectra of the dimer, deconvolution of visible absorption spectra of Boc−(Por^{Zn,S})$_n$−OBu^t (n = 1, 2, 4, and 8), effect of condensation number n of Boc−(Por^{Zn,S})$_n$−OBu^t on fluorescence yield, effect of ligands other than en, effect of en on the fluorescence intensity of the monomer, stepwise change of the dimer spectrum upon addition of en, definition of (R, Θ, Φ, ϕ, θ, Ψ), and specific distribution of the nearest-neighbor Chls in natural organs. This material is available free of charge via the Internet at http://pubs.acs.org.

JA809851D